

# Journal of Materials Chemistry A

Accepted Manuscript



This is an *Accepted Manuscript*, which has been through the Royal Society of Chemistry peer review process and has been accepted for publication.

*Accepted Manuscripts* are published online shortly after acceptance, before technical editing, formatting and proof reading. Using this free service, authors can make their results available to the community, in citable form, before we publish the edited article. We will replace this *Accepted Manuscript* with the edited and formatted *Advance Article* as soon as it is available.

You can find more information about *Accepted Manuscripts* in the [Information for Authors](#).

Please note that technical editing may introduce minor changes to the text and/or graphics, which may alter content. The journal's standard [Terms & Conditions](#) and the [Ethical guidelines](#) still apply. In no event shall the Royal Society of Chemistry be held responsible for any errors or omissions in this *Accepted Manuscript* or any consequences arising from the use of any information it contains.

# Polyaniline Nanofiber/Vanadium Pentoxide Sprayed Layer-by-Layer Electrodes for Energy Storage

Cite this: DOI: 10.1039/x0xx00000x

Lin Shao,<sup>a</sup> Ju-Won Jeon<sup>b</sup> and Jodie L. Lutkenhaus<sup>b</sup>

Received 00th January 2012,  
Accepted 00th January 2012

DOI: 10.1039/x0xx00000x

www.rsc.org/

Layer-by-layer assembly, as a low-cost process to create high-performance coatings, has been widely studied over the past 20 years. However, conventional layer-by-layer assembly is not well suited to large-area, large-scale and rapid application because of the long time scale required to complete a multilayer coating. Here, we develop a simple, water-based, rapid spray-on method to produce and prepare polyaniline/vanadium pentoxide layer-by-layer thin film cathodes for Li-ion batteries. This method uses spray-assisted LbL assembly, which is suitable to coating over large areas rapidly. The result is a water-processable hybrid cathode with high capacity (up to 232 mAh/g at a discharge current of 5  $\mu\text{A}/\text{cm}^2$ ), specific energy (up to 650 mWh/g at a discharge current of 0.5  $\mu\text{A}/\text{cm}^2$ ), specific power (up to 3395 mW/g at a discharge current of 25  $\mu\text{A}/\text{cm}^2$ ), and good cycle life. The performance is dependent on thickness and discharge rate. Compared to the traditional polyaniline/vanadium pentoxide prepared by dipping at a rate of 0.0373 nm/sec, sprayed electrodes grow at a significant high rate of 0.42 nm/sec – 11 times faster. This approach demonstrates the rapid layer-by-layer assembly of Li-ion battery electrodes without sacrificing performance.

## Introduction

New breakthroughs in electrodes are urgently needed in order to develop high-performance Lithium-ion batteries,<sup>1, 2</sup> especially with regard to emerging applications such as thin film, paintable, or flexible batteries. Layer-by-layer (LbL) assembly is a promising processing technique in this arena because the resulting (LbL) electrodes fit many potential needs (control over film thickness, conformal deposition onto a variety of surfaces, molecular mixing of dissimilar materials, *etc.*). Herein, we present the rapid fabrication of LbL cathodes via alternate spraying of polyaniline nanofibers (PANI NFs) and  $\text{V}_2\text{O}_5$  in a water-based process suitable for large-area deposition. Up to now, PANI NF/ $\text{V}_2\text{O}_5$  LbL cathodes have been assembled only via dipping, which is a slow, cumbersome process. Importantly, it is not well established if these LbL electrodes made via spraying are substantially different from those made via dipping.

Polyaniline (PANI), a p-type conjugated polymer, is a promising cathode material for electrochemical energy storage because of its relatively good processability, low monomer cost, and adjustable chemical and physical properties.<sup>3-9</sup> Nanostructured PANI (*e.g.* nanotubes,<sup>10</sup> nanowires,<sup>11</sup> nanofibers,<sup>12</sup> nanospheres<sup>13</sup> and nanodrites<sup>14</sup>) and PANI-complexes, such as PANI:polyacid, have received great interest.<sup>15, 16</sup> Charge is stored through reversible doping and oxidation (or dedoping and reduction), yielding a

theoretical capacity of 147 mAh  $\text{g}^{-1}$  (excluding the dopant's mass) when switching between leucoemeraldine base and emeraldine salt forms. PANI's conductivity can be as high as 50-4200 S/cm, depending on the preparation process.<sup>17, 18</sup> PANI NFs are particularly interesting for battery cathodes because they offer conductivity as well as porosity and high surface area.<sup>12</sup>

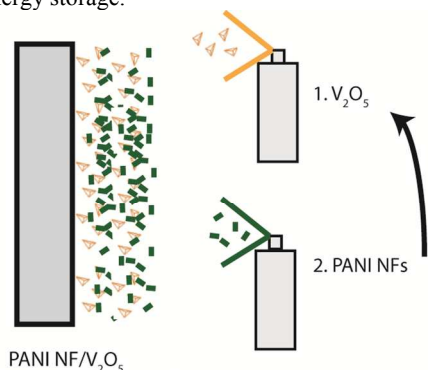
$\text{V}_2\text{O}_5$  is another interesting cathode material for Lithium-ion batteries because of its high theoretical capacity of 511 mAh  $\text{g}^{-1}$  (assuming  $x = 4$  for  $x\text{Li}^+ + xe^- + \text{V}_2\text{O}_5 \rightarrow \text{Li}_x\text{V}_2\text{O}_5$ ). However,  $\text{V}_2\text{O}_5$  suffers from extreme volumetric expansion during cycling, slow ion diffusion, and low electronic conductivity,<sup>19, 20</sup> which has limited its practical application. Nanostructured  $\text{V}_2\text{O}_5$ <sup>21, 22</sup> has been proposed as one means of addressing volumetric expansion. Different processes towards the fabrication of PANI/ $\text{V}_2\text{O}_5$  hybrid electrodes have been proposed (in-situ polymerization,<sup>23, 24</sup> casting,<sup>25</sup> and LbL assembly<sup>26-30</sup>), yielding varying degrees of success towards enhancement of conductivity and ion transport.

Recently, we reported the synthesis of PANI/ $\text{V}_2\text{O}_5$  and PANI NF/ $\text{V}_2\text{O}_5$  composite electrodes via dip-assisted LbL assembly,<sup>31, 32</sup> which showed good performance as thin film cathodes. LbL assembly is the sequential adsorption of oppositely charged materials such as polyelectrolytes, organic, and inorganic colloids.<sup>33, 34</sup> Positively charged PANI and negatively charged  $\text{V}_2\text{O}_5$  were alternately adsorbed from water to a current collector to form a thin film cathode via dipping. A film thickness of 1.2  $\mu\text{m}$  yielded

optimum results, with a discharge capacity and specific energy of 320 mAh/g and 886 mWh/g at a current of 0.5  $\mu\text{A}/\text{cm}^2$ , respectively, as well as a specific power of 4000 mW/g at a discharge current of 25  $\mu\text{A}/\text{cm}^2$ . This dip-assisted LbL process requires 30 minutes per cycle, translating to a growth rate of 0.0373 nm/sec. Although promising, it is desired to produce these electrodes more rapidly and to increase the electrode's thickness.

An alternative technique, automated spray-assisted LbL assembly, has been developed to speed up the deposition of LbL thin films.<sup>35,36</sup> Oppositely charged species are alternately sprayed onto a substrate. The diffusion path of molecules from the solution to the substrate is decreased by strong convection resulting from spraying, which leads to a significant reduction in the contact time required to deposit films.<sup>37,38</sup> Since then, numerous research groups have explored this alternative processing approach in many applications such as antireflection coatings.<sup>39,40</sup> However, few studies have focused upon energy storage using automated spray-assisted LbL assembly.<sup>19,38</sup> Spraying is also of interest because it allows for the deposition of battery electrodes onto unconventional substrates such as fabrics, structural panels, windows, etc.

In this work, we demonstrate porous PANI NF/ $\text{V}_2\text{O}_5$  LbL electrodes made via spray-assisted LbL assembly, Figure 1. Of special interest is how these films compare against those made by dip-assisted LbL assembly in terms of structure, properties, and electrochemical performance. First, we present explore best practices in translating this system from dip to spray, which yields a unique challenge arising from difficulties in spraying nanofibers. Second, the electrochemical performance of spray-assisted LbL electrodes is quantified using cyclic voltammetry and galvanostatic cycling. Lastly, electrodes made via spray are compared to those made via dip. The work presented thus forth provides a framework for how to translate an LbL system from dip to spray, how to address issues with spraying nanoparticles, and how to fabricate sprayed electrodes for energy storage.



PANI NF/ $\text{V}_2\text{O}_5$   
Spray-Assisted LbL Electrode

**Figure 1.**  $\text{V}_2\text{O}_5$  and PANI NF suspensions are alternately sprayed onto a substrate to build up a spray-assisted LbL electrode.

## Experimental section

**Materials:** Aniline, ammonium peroxydisulfate, lithium perchlorate and propylene carbonate were purchased from Sigma Aldrich. Vanadium triisopropoxide oxide was purchased from Gelest, Inc. Linear polyethylenimine (PEI, Mw~25,000) and poly(acrylic acid) (PAA, Mw~50,000, 25% aqueous solution) were purchased from Polysciences. Lithium foil was purchased from Alfa Aesar. Indium-tin oxide (ITO)-coated glass (resistance <20  $\Omega$ ) was purchased from Delta Technologies. Molecular porous membrane tubing (Molecular weight cut-off = 12-14,000 Daltons) was purchased from Spectrum Labs. All materials were used as received.

**Polyaniline nanofiber synthesis and dispersion preparation:** PANI nanofibers were synthesized following a published procedure.<sup>41</sup> Ammonium peroxydisulfate (0.915 g, 4 mmol) and aniline (1.49 g, 16 mmol) were dissolved in HCl solution (1 M, 50 mL), respectively. Both solutions were purged using argon for 1 h at room temperature. Then, these two solutions were rapidly mixed under argon and stirred for 24 h at room temperature, resulting in a green dispersion of PANI nanofibers. The dispersion was dialyzed in 18.2 M $\Omega$  deionized water for three days; the water was changed twice each day. The dispersion was then diluted with water to 400 mL, and the pH value was adjusted to 2.5 using HCl. In order to stabilize the PANI dispersion and reduce the aggregation of PANI nanofibers, sodium dodecyl sulfate was added with a concentration of 0.05 wt%. After 3 h sonication, the PANI nanofiber dispersion was ready for use. Based on the yield calculated by Yun group,<sup>42</sup> this dispersion had a concentration of 0.5 mg/mL.

**Vanadium pentoxide synthesis and dispersion preparation:**  $\text{V}_2\text{O}_5$  was prepared using a published sol-gel method.<sup>26,31,43</sup> Briefly, vanadium triisopropoxide oxide (1 mL) was added to 500 mL deionized water. The mixture was concentrated to 250 mL using rotary evaporation at 60°C, yielding an orange mixture of 0.022 M elemental vanadium at pH 2.5. According to the phase diagram reported by Livage group,<sup>44</sup> the vanadium species in this mixture is mainly  $\text{V}_{10}\text{O}_{26}(\text{OH})_2^{4-}$ .

**Preparation of PANI nanofiber/ $\text{V}_2\text{O}_5$  spray LbL films:** Sprayed LbL films were fabricated on ITO-coated glass using an automated spray-LbL system (Svaya Nanotechnologies). ITO-coated glass substrates were cleaned via sonication in dichloromethane, acetone, methanol, and deionized water for 15 min each. After cleaning, all substrates were dried in a convection oven at 50°C, followed by 5-min oxygen plasma treatment (Harrick PDC-32G).<sup>45</sup> Two layer pairs of PEI and PAA were sprayed onto the clean substrates to improve the growth of LbL films.<sup>30</sup> Briefly, 20 mM PEI solution with pH 4 was sprayed for 10 s followed by spray-rinsing by water with pH 4 for 10 s, and then the same process was performed with pH 4, 20 mM PAA solution followed by the same rinsing step. Right after the deposition of these prelayers, PANI nanofiber/ $\text{V}_2\text{O}_5$  LbL films were constructed using the automated spray-LbL system. PANI nanofiber dispersion was sprayed for 10 s followed by 1 min of blow-drying using air at 25 psi. The same procedure was then followed by exposure to  $\text{V}_2\text{O}_5$  solution and blow-drying as before. All spray solutions were delivered using air regulated to 25 psi. Films were designated as (PANI nanofiber/ $\text{V}_2\text{O}_5$ )<sub>n</sub>, where the subscript *n* denotes the number of layer pairs. LbL films were dried in ambient air following assembly.

**Materials characterization:** UV-Vis absorption spectra of PANI nanofiber/ $\text{V}_2\text{O}_5$  spray-assisted LbL films on ITO-coated glass slides were recorded using a Hitachi U-4100 spectrophotometer. Zeta potential of PANI nanofibers dispersed in water was measured using Nano ZS90, Malvern Instruments. The thickness of the sprayed films was measured using a P-6 profilometer (KLA-Tencor). The thickness of each sample was the average of at least ten measurements. The mass growth of the sprayed films was measured using a quartz crystal microbalance (Maxtek-RQCM, Inficon). X-ray photoelectron spectroscopy (XPS), (Kratos Axis Ultra DLD) was used to investigate the composition of the sprayed films' surface. The instrument used a monochromatic Al X-ray source at a pass energy of 40 eV and a charge neutralizer. The analyzed area was 700×300  $\mu\text{m}$ . The take off angle was 90 degrees, and the acceleration voltage was 12 kV. The surfaces of the sprayed LbL films and drop-cast PANI NFs was imaged using scanning electron microscopy (SEM, JEOL JSM-7500F) and the morphology of drop-cast  $\text{V}_2\text{O}_5$  films was investigated using transmission electron microscopy (TEM, JEOL 2010).

**Electrochemical characterization:** Sprayed films were dried in air for 24 h after they were fabricated. Then these films were dried under vacuum for 10 min and immersed in electrolyte in the glovebox for 1 hr prior to the electrochemical tests. Electrochemical properties of PANI NF/V<sub>2</sub>O<sub>5</sub> spray-assisted LbL films were investigated using either a three-electrode cell or a two-electrode sandwich cell in an oxygen-free, water-free, argon-filled glove box (MBraun). For the three-electrode cell, the sprayed film was the working electrode, and two lithium ribbons served as counter and reference electrodes. For the two-electrode cell, the sprayed film was the working electrode, and lithium ribbon served as counter and reference electrode. The electrolyte was 0.5 M LiClO<sub>4</sub> in propylene carbonate. Cyclic voltammetry and galvanostatic charge/discharge testing were performed at room temperature using a Solartron SI 1287 in a voltage range of 2~3.5 V (cyclic voltammetry) and 2.5~3.5 V (charge/discharge testing) versus Li/Li<sup>+</sup>. Electrochemical impedance spectroscopy (EIS, Gamry) was carried out in a two-electrode cell at 2, 2.75, and 3.5 V vs. Li/Li<sup>+</sup> between 1 mHz and 1000 mHz with an amplitude of 10 mV. Capacity, energy, and power are reported on a basis of total electrode mass.

## Results and Discussion

### Spray-LbL assembly of PANI and V<sub>2</sub>O<sub>5</sub>

The primary target of this work was to fabricate relatively thick PANI/V<sub>2</sub>O<sub>5</sub> electrodes efficiently and rapidly using a scalable spray-assisted LbL assembly process translated from dip-assisted LbL assembly. Conventional dip-assisted LbL assembly proceeds at 30 min per layer pair for PANI-containing systems,<sup>31, 46, 47</sup> and relies on diffusion of species from bulk solution to the substrate's surface. On the other hand, spray-assisted LbL assembly significantly reduces the diffusion path of the adsorbing species to that of the thickness of the wetting layer that forms during spraying.<sup>48</sup> For spray-assisted LbL assembly, operation parameters such as spray distance, drain time, blow-drying time, concentration, and pressure have significant influence on the growth of LbL electrodes. Of these parameters, we have found that blow-drying time and concentration are most sensitive for the PANI/V<sub>2</sub>O<sub>5</sub> system.

PANI NFs and V<sub>2</sub>O<sub>5</sub> were alternately sprayed onto glass slides for varying blow-drying times. Drop-cast PANI NFs, imaged using scanning electron microscopy (SEM), were 30 to 50 nm in diameter and 100 to 500 nm in length, Figure 2a. V<sub>2</sub>O<sub>5</sub> fibers, observed using transmission electron microscopy (TEM), were 200 nm in diameter and 1.5 μm in length, Figure 2b.

Blow-drying increases convection, and reduces the thickness of the wetting layer, leading to a reduced diffusion path. As the period of blow-drying increases, water evaporates from the wetting layer, further reducing the path. For example, if the blow-drying time was increased from 30 sec to 1 min, the thickness of a sample with 50 layer pairs increased from 1 μm to 3 μm, Figure S1. However, further increasing the blow-drying time did not appreciably affect growth. The importance of blow-drying time highlights the general difficulty in forming robust coatings via spraying, particularly for high aspect ratio nanoparticles. Elsewhere, it has been illustrated that the anisotropy of carbon nanotubes leads to minimal contact between oppositely charged species, and the rigid nature of the nanotubes

impedes the translational and rotational movements and elastic deformations that would otherwise promote contact.<sup>38</sup> Blow-drying time is a means of forcing adsorption to overcome slow translational and rotational movement. Air pressure was also explored, but had little effect on the growth rate.

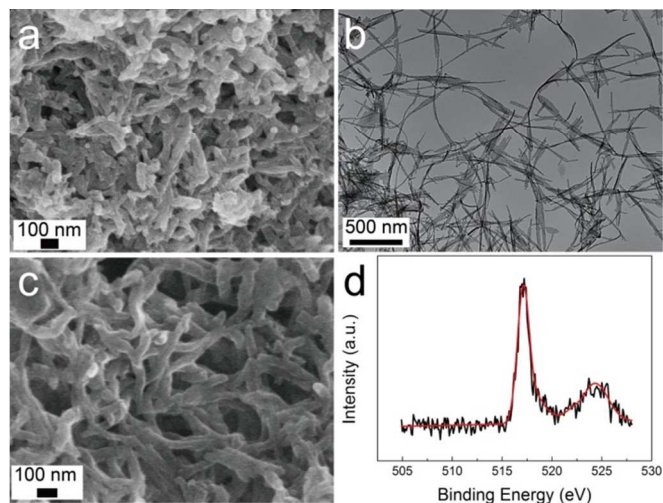


**Figure 2.** (a) SEM image of drop-cast PANI NFs and (b) TEM image of V<sub>2</sub>O<sub>5</sub>; (c) SEM of a (PANI NF/V<sub>2</sub>O<sub>5</sub>)<sub>30</sub> spray-assisted LbL assembly; (d) XPS of a (PANI NF/V<sub>2</sub>O<sub>5</sub>)<sub>30</sub> spray-assisted LbL film for the V2p region.

The effect of concentration on film growth and uniformity was also explored, Figure S2. It has been shown for conventional dip-assisted LbL assembly that increasing the polyelectrolyte concentration (up to a certain point) decreases the adsorption time to saturation. However, the opposite was found here for spraying of polyaniline nanofibers. PANI NF/V<sub>2</sub>O<sub>5</sub> spray-assisted LbL samples were made using a PANI NF suspension bearing concentrations of either 0.5 or 1 mg/mL. We found that films assembled at the higher concentration exhibited poor growth and uniformity. This observation is tied to the aggregation of PANI NFs at higher concentrations, which impedes LbL growth. By decreasing the concentration of PANI NFs to 0.5 mg/mL, good film growth and uniformity could be obtained. Because of their smaller diameter, we have found that V<sub>2</sub>O<sub>5</sub> is much easier to spray and aggregation is far less of an issue.

By selecting a blow drying time of 1 min and a concentration of 0.5 mg/mL PANI NF, sprayed electrodes grew at a significant higher rate of 0.42 nm/sec, which is 11 times faster than conventional dip-assisted LbL assembly. The surface of (PANI NF/V<sub>2</sub>O<sub>5</sub>)<sub>30</sub> spray-LbL films with V<sub>2</sub>O<sub>5</sub> as the outermost layer is shown in Figure 2c, in which the subscript “30” indicates that 30 layer pairs were deposited. The morphology was similar to that of the drop-cast PANI NFs. Due to the smaller size of V<sub>2</sub>O<sub>5</sub> relative to PANI NFs, it was difficult to observe V<sub>2</sub>O<sub>5</sub> distinctly under SEM.

X-ray photoelectron spectroscopy was carried out to confirm the existence of V<sub>2</sub>O<sub>5</sub> within the spray-assisted LbL assembly and to

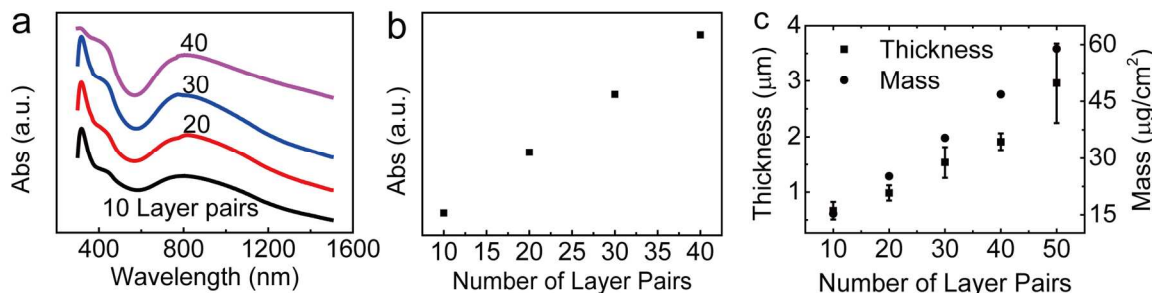


**Figure 3.** (a) UV-Vis spectra of PANI NF/ $V_2O_5$  spray-assisted LbL films; (b) Absorbance at 825 nm as a function of number of layer pairs; (c) Growth profile (thickness and mass) of PANI NF/ $V_2O_5$  spray-assisted LbL films measured using profilometry and QCM. Error bars represent standard deviation across multiple measurements.

determine its relative abundance, Figure 2d. Two peaks at 517.4 and 524.7 eV were observed and assigned to the  $2p_{3/2}$  and  $2p_{1/2}$  orbitals, respectively, corresponding to the  $V^{5+}$  oxidation state.<sup>24</sup> The ratio of V to N was 44:56 at the film's surface, which translated to 54 wt%  $V_2O_5$  and 46 wt% PANI NF.

As the number of layer pairs increased, the PANI NF/ $V_2O_5$  LbL electrodes became darker and thicker, Figure S3 and Figure 3. UV-Vis spectra were collected every ten layer pairs; peaks associated with PANI were clearly visible, dominating over  $V_2O_5$ , as we have observed before.<sup>31, 46</sup> The characteristic peak of PANI's emeraldine salt oxidation state shifted to lower wavelengths from 900 nm (PANI NF) to 800 nm (PANI NF in the spray-assisted LbL film) because of strong interactions between PANI NFs and  $V_2O_5$ , Figure 3a. The absorbance at 825 nm increased linearly with the increasing number of layer pairs, Figure 3b. This linear growth was also confirmed using profilometry (59 nm per layer pair) and quartz crystal microbalance ( $1.2 \mu\text{g cm}^{-2}$  per layer pair) (Figure 3c). The average density of the LbL film, estimated from the mass and thickness growth profiles, was  $0.21 \text{ g cm}^{-3}$ . This low density was indicative of the very porous nature of the LbL film. From the density of polyaniline ( $1.329 \text{ g cm}^{-3}$ ),  $V_2O_5$  ( $3.36 \text{ g cm}^{-3}$ ) and the polyaniline nanofiber/ $V_2O_5$  LbL assembly, the porosity of the LbL film's porosity was estimated to be 90%. This value is slightly higher than that of analogous films made via dipping, for which the porosity was 85 %.<sup>32</sup>

### Energy storage in PANI NF/ $V_2O_5$ LbL electrodes

The electrochemical properties of (PANI NF/ $V_2O_5$ )<sub>n</sub> spray-assisted LbL films were initially investigated using a three-electrode cell. This system was subjected to cyclic voltammetry and galvanostatic charge-discharge and cycling tests. PANI NFs are oxidized/reduced between leucoemeraldine base and emeraldine salt via doping and dedoping of anions, and  $V_2O_5$  undergoes intercalation and deintercalation as charge is transferred.

### Cyclic voltammetry

Cyclic voltammetry of (PANI NF/ $V_2O_5$ )<sub>30</sub> spray-assisted LbL films was performed in the voltage range of 2–3.5 V vs.  $\text{Li/Li}^+$  at scan rates varying from 1 to 20 mV/s, Figure 4a. Two

oxidation/reduction pairs were present in anodic and cathodic scans, Figure 4a inset. The symmetry of both peaks and their minimal drift in potential with respect to scan rate was indicative of the chemical reversibility of this hybrid system. In the anodic scan, the broad shoulder centered around 2.68 V and the peak at 3 V was attributed to  $V_2O_5$  and PANI NFs, respectively. As the scan rate increased, the oxidation peak attributed to PANI NFs grew in dominance relative to  $V_2O_5$ 's oxidation shoulder. At higher potentials (3–3.5 V), a capacitive plateau attributed to PANI NFs was observed. These results indicate that both PANI NFs and  $V_2O_5$  are electrochemically active within the thin film electrode. The peak current scaled with the square root of the scan rate, indicative of a diffusion-limited redox reaction.

To assess charge storage as it varies with electrode thickness, electrodes of varying layer pairs were assessed at a fixed scan rate of 1 mV/s, Figure 4b. The low voltage peak, attributed to  $V_2O_5$ , grew in dominance over the PANI redox peak as the number of layer pairs increased, possibly because less PANI was participating in reduction/oxidation as compared to  $V_2O_5$ . The peak current at 3 V increased linearly with the number of layer pairs, Figure 4c, which indicates electrochemical accessibility throughout the film for those up to 3  $\mu\text{m}$  thick. In contrast, analogous electrodes made via dip-assisted LbL films demonstrated strong diffusion limitations for thicknesses above 1.7  $\mu\text{m}$ , such that a significant portion of the material was inactive. We attribute the superior response of the spray-assisted LbL electrodes to its higher porosity.

As the electrode was reduced and oxidized, its color changed from dark green to clear. To assess the electrode's electrochromism, UV-vis spectroscopy was performed over varying potentials, Figure S4. UV-vis spectra indicate that the electrochromic activity was dominated by PANI nanofibers, presumably because the extinction coefficient of  $V_2O_5$  is much smaller than that of PANI over the visible region.<sup>49, 50</sup> A spray-assisted LbL electrode held at 3.5 V vs.  $\text{Li/Li}^+$  had a broad peak at 850 nm, which disappeared for the sample held at 2.0 V. Such behavior is typical for PANI, which is green as emeraldine salt and uncolored as leucoemeraldine base for 3.5 and 2.0 V, respectively.

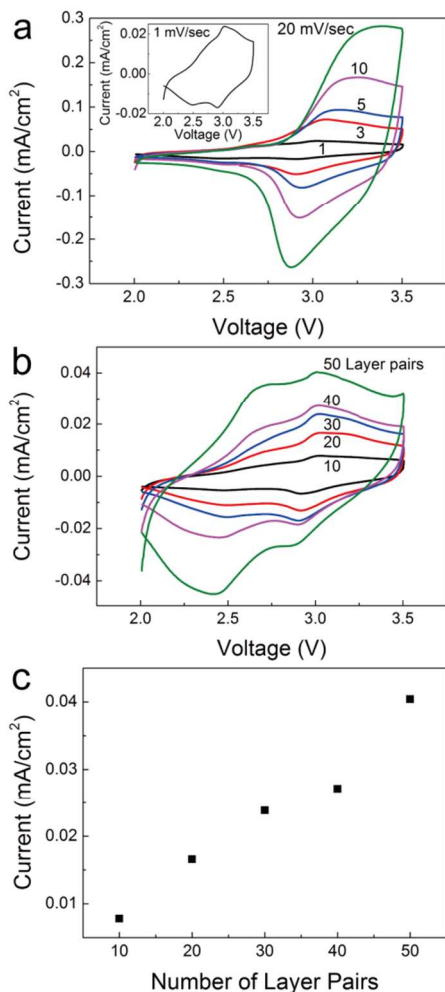


**Figure 4.** Cyclic voltammograms of (a) (PANI NF/V<sub>2</sub>O<sub>5</sub>)<sub>30</sub> spray-assisted LbL electrodes with different scan rates and of (b) (PANI NF/V<sub>2</sub>O<sub>5</sub>)<sub>n</sub> LbL films with varying number of layer pairs at a constant scan rate of 1 mV/s; (c) current at 3 V versus layer pair number using data from (b). Potential is vs. Li/Li<sup>+</sup>. Electrolyte is 0.5 M LiClO<sub>4</sub> in propylene carbonate and all experiments performed under inert atmosphere.

#### Charge/discharge testing

Galvanostatic charge/discharge testing was performed to investigate the behavior of the spray-assisted LbL electrodes between 2.5 and 3.5 V. A wider voltage range obviously increases the capacity of these LbL film electrodes, but polyaniline irreversibly oxidizes to pernigraniline base above 3.5 V and V<sub>2</sub>O<sub>5</sub> irreversibly forms the  $\gamma$ -Li<sub>x</sub>V<sub>2</sub>O<sub>5</sub> phase below 2 V.<sup>51</sup> The charge/discharge profile of (PANI NF/V<sub>2</sub>O<sub>5</sub>)<sub>30</sub> spray-assisted LbL films is illustrated in Figure 5a. The sloping discharge profile is typical of a conjugated polymer.<sup>5</sup> As expected, the capacity increases from 104 to 125 mAh g<sup>-1</sup> with decreasing discharge current from 20 to 5  $\mu$ A cm<sup>-2</sup>.

The capacity was found to increase substantially with thickness, Figure 5b. The largest capacity of (PANI NF/V<sub>2</sub>O<sub>5</sub>)<sub>n</sub> spray-LbL films was 232 mAh/g at a current of 5  $\mu$ A/cm<sup>2</sup> and  $n=50$ , which was nearly 3  $\mu$ m thick. However, this capacity-thickness relationship is contrary to that of the samples prepared by traditional dip-assisted LbL assembly, in which capacity was limited for thicker electrodes.<sup>32</sup> Again, the higher porosity of spray-assisted LbL

assembly might explain its enhanced charge/discharge behavior relative to analogous dip-LbL electrodes. By translating the PANI NF/V<sub>2</sub>O<sub>5</sub> LbL system from dip to spray, performance is maintained in electrodes twice as thick as compared to those made by dipping.

Cycling was performed to assess the cathode's stability, Figure 5c. The capacity of (PANI/V<sub>2</sub>O<sub>5</sub>)<sub>30</sub> LbL electrodes decreased 17% after 100 cycles. After cycling, UV-vis spectra of the sample demonstrated that a small amount of pernigraniline base had formed, which is a common mechanism of degradation associated with polyaniline.<sup>32</sup> We consider this electrode's cyclability good compared to our previous investigations, in which degradation proceeded more rapidly. This good cycling behavior here is attributed to the porous morphology, which alleviated volumetric expansion and reduced the diffusion path of ions.

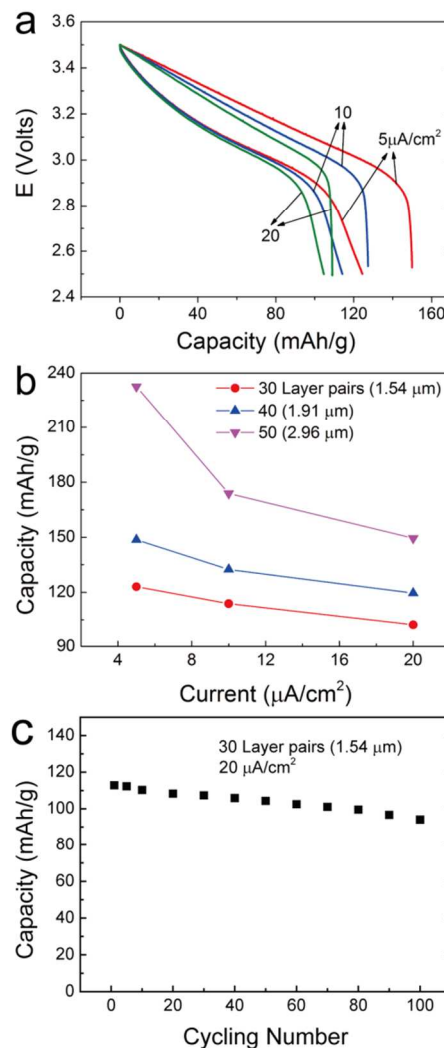


**Figure 5.** (a) Galvanostatic charge and discharge profiles for (PANI/V<sub>2</sub>O<sub>5</sub>)<sub>30</sub> spray-assisted LbL electrodes; (b) Capacity vs. discharge current for spray-assisted LbL electrode of varying thickness; (c) Capacity vs. number of cycles for (PANI/V<sub>2</sub>O<sub>5</sub>)<sub>30</sub> LbL electrodes.

Galvanostatic cycling at varying discharge currents was carried out to estimate the rate capability of (PANI NF/V<sub>2</sub>O<sub>5</sub>)<sub>30</sub> spray-assisted LbL electrodes, Figure 6a. A stable capacity of 189 mAh/g was attained at a current of 0.5  $\mu$ A/cm<sup>2</sup>. As the discharge current increased to 25  $\mu$ A cm<sup>-2</sup>, the capacity decreased to 43% of its initial

value, and the capacity recovered upon returning to  $0.5 \mu\text{A}/\text{cm}^2$ . Compared to the  $(\text{PANI NF}/\text{V}_2\text{O}_5)_{16}$  dip-LbL electrode, the  $(\text{PANI NF}/\text{V}_2\text{O}_5)_{30}$  spray-assisted LbL electrode has a better rate capability as evidenced by Figure 6a in that its capacity is less sensitive to discharge current.

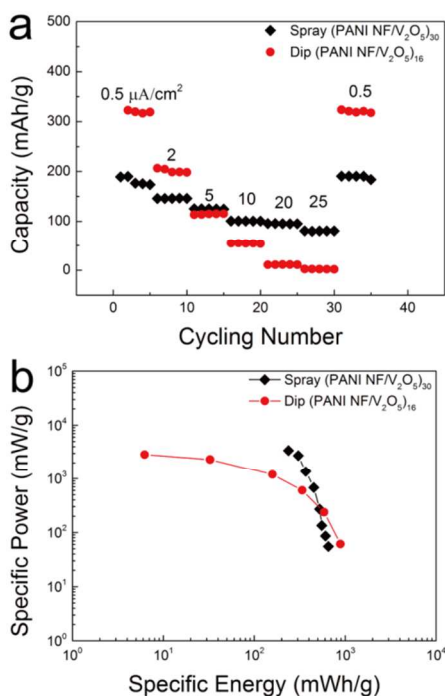


**Figure 6.** (a) Galvanostatic cycling and (b) Ragone plot of  $(\text{PANI NF}/\text{V}_2\text{O}_5)_{30}$  spray-assisted LbL electrodes and  $(\text{PANI NF}/\text{V}_2\text{O}_5)_{16}$  dip-assisted LbL electrodes. The number of layer pairs was selected such that the electrodes would bear similar thicknesses of  $1.2 \mu\text{m}$ .

The specific power and energy were calculated and summarized in a Ragone plot, Figure 6b. At high discharge rates, the spray-assisted LbL electrode possessed a higher specific energy and a similar power as compared to the dip-assisted LbL electrode. This observation is attributed to the higher porosity of the spray-assisted LbL samples (90%) as compared to that of the dip-assisted LbL samples (85%).<sup>32</sup> For the spray-assisted LbL electrode, the highest specific energy measured was  $650 \text{ mWh/g}$  at a discharge current of  $0.5 \mu\text{A}/\text{cm}^2$  and the highest specific power was  $3395 \text{ mW/g}$  at a discharge current of  $25 \mu\text{A}/\text{cm}^2$ . In comparison,  $\text{PANI NF}/\text{V}_2\text{O}_5$  LbL electrodes prepared by dipping achieved a specific energy of  $867 \text{ mWh/g}$  at a discharge current of  $0.5 \mu\text{A}/\text{cm}^2$  and a specific power of  $2853 \text{ mW/g}$  at a discharge current of  $25 \mu\text{A}/\text{cm}^2$ .

The volumetric capacity, energy, and power were estimated from the porosity and composition of the electrode. The spray-assisted LbL electrode demonstrated higher capacities at lower discharge currents ( $80 \text{ mAh}/\text{cm}^3$  at  $0.5 \mu\text{A}/\text{cm}^2$ ), Figure S5. On the other hand, the spray-assisted LbL electrode had better rate capability, maintaining a capacity of  $20\text{--}40 \text{ mAh}/\text{cm}^3$  over a broad range of discharge currents ( $0.5\text{--}25 \mu\text{A}/\text{cm}^2$ ). These results are also reflected in volumetric Ragone plots, Figure S6, in which the spray-assisted LbL electrodes exhibit a higher power density relative to dip-assisted LbL electrodes. These results confirm that a small increase in porosity (from 85 to 90% for dip to spray) can have a large impact on rate capability and power.

## Electrochemical Impedance spectroscopy

Electrochemical impedance spectroscopy was applied to determine how the electrode's conductivity varies as it is reduced and oxidized, Figure 7. The conductivity of PANI NFs is determined by the oxidation state and the degree of doping, which vary with potential. As the  $(\text{PANI NF}/\text{V}_2\text{O}_5)_{30}$  spray-assisted LbL film is oxidized, the shape of the impedance spectra clearly changes, especially in the low frequency region. At low voltages such as 2 and  $2.75 \text{ V}$ , PANI NFs were in the reduced state, leucoemeraldine base; the corresponding Nyquist plots consisted of a semicircle in the high frequency region, a distorted semicircle in the medium frequency region, and a straight line in the low frequency region.<sup>52</sup> Upon increasing the voltage to  $3.5 \text{ V}$ , PANI NFs oxidized to emeraldine salt, and the distorted semicircle evolved into a distinct semicircle; further, the straight line in the low frequency region changed to a near-vertical line, indicating the electrode's conductive nature.<sup>52</sup> In order to quantitatively analyze the impedance spectra of the spray-assisted LbL electrodes, an equivalent-circuit model was applied shown in Figure 7 inset. Similar models have been reported by Hung *et al.* and Hu *et al.*<sup>52, 53</sup> The best-fit values for the equivalent-circuit's elements are shown in Table S1.  $R_2$ , representing the bulk electron-hopping resistance, decreased from  $350.3$  to  $228.2 \Omega$  upon oxidation from  $2.0$  to  $3.5 \text{ V}$ , which corresponds into the electrodes decreased resistance and increased conductivity.

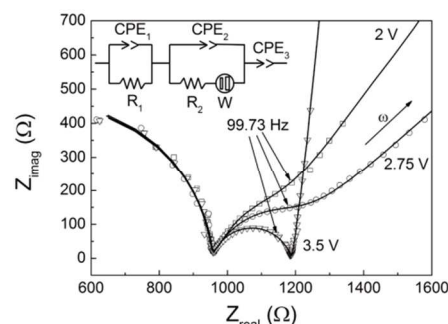


**Figure 7.** Nyquist plots of (a)  $(\text{PANI NF}/\text{V}_2\text{O}_5)_{30}$  spray-assisted LbL electrodes at different voltages. Symbol: experimental values, Line: fitting of the equivalent-circuit model to the data.

## Conclusions

Sprayed hybrid  $\text{PANI NF}/\text{V}_2\text{O}_5$  LbL electrodes for electrochemical energy storage were successfully fabricated in rapid and scalable manner. It was found that blow-drying time and concentration are most critical in translating the  $\text{PANI NF}/\text{V}_2\text{O}_5$  system from dip to spray, as it controls the thickness of the wetting layer and aggregation. The growth rate of the spray-assisted LbL films was  $.42 \text{ nm}/\text{sec}$  and 11 times faster than dip-assisted LbL assembly. The porous morphology resulted in good rate capability, cycle life, high specific power and energy. No discernable drawbacks in performance were observed for spraying as compared to dipping. For the spray-assisted LbL electrode, the highest specific energy measured was  $650 \text{ mWh/g}$  at a discharge current of  $0.5 \mu\text{A}/\text{cm}^2$  and the highest specific power was  $3395 \text{ mW/g}$  at a discharge current of  $25 \mu\text{A}/\text{cm}^2$ . In comparison,  $\text{PANI NF}/\text{V}_2\text{O}_5$  LbL electrodes prepared by dipping achieved a specific energy of  $867 \text{ mWh/g}$  at a discharge current of  $0.5 \mu\text{A}/\text{cm}^2$  and a specific power of  $2853 \text{ mW/g}$  at a discharge current of  $25 \mu\text{A}/\text{cm}^2$ . Both PANI NFs and  $\text{V}_2\text{O}_5$  participated in charge storage, and conductivity varied with respect to PANI's oxidation state.

In the future, we seek to further scale the spray-assisted LbL assembly process to thicker electrodes, large surface areas, unconventional substrates (textiles, flexible plastic, etc.) in the pursuit of flexible or structural energy storage. LbL assembly may be particularly important in this area of thin film batteries because it allows the uniform deposition of electrode materials onto a variety of surfaces.

## Acknowledgements

This work is supporting in part by the National Science Foundation (Grant No. 1336716) and the Air Force Office of Sponsored Research (FA-9550-12-1-0147). We thank Dr. Nicole Zacharia for profilometer and FTIR spectrometer access, and Dr. Akbulut for DLS and zetapotential access. We also thank the TAMU Materials Characterization Facility.

## Notes and references

<sup>a</sup> Department of Chemical & Environmental Engineering

Yale University

New Haven, Connecticut 06511. USA

<sup>b</sup> Artie McFerrin Department of Chemical Engineering

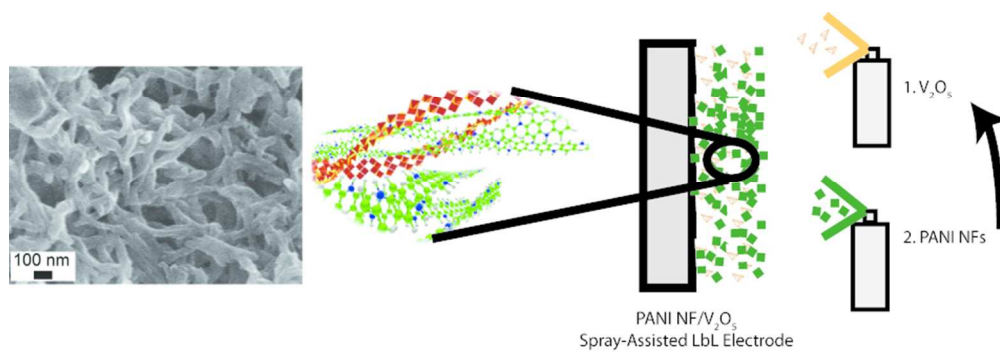
Texas A&M University

College Station, Texas 77843. USA

E-mail: jodie.lutkenhaus@che.tamu.edu

Electronic Supplementary Information (ESI) available: See DOI: 10.1039/b000000x/

- J. B. Goodenough and Y. Kim, *Journal of Power Sources*, 2011, **196**, 6688-6694.
- H. Li, Z. Wang, L. Chen and X. Huang, *Advanced Materials*, 2009, **21**, 4593-4607.
- A. G. Macdiarmid and A. J. Epstein, *Synthetic Metals*, 1994, **65**, 103-116.
- V. I. Krinichnyi, *Russian Chemical Bulletin*, 2000, **49**, 207-233.
- P. Novak, K. Muller, K. S. V. Santhanam and O. Haas, *Chemical Reviews*, 1997, **97**, 207-281.
- S. Bhadra, D. Khastgir, N. K. Singha and J. H. Lee, *Progress in Polymer Science*, 2009, **34**, 783-810.
- G. A. Snook, P. Kao and A. S. Best, *Journal of Power Sources*, 2011, **196**, 1-12.
- J. F. Mike and J. L. Lutkenhaus, *ACS Macro Letters*, 2013, **2**, 839-844.
- J. F. Mike and J. L. Lutkenhaus, *Journal of Polymer Science Part B: Polymer Physics*, 2013, **51**, 468-480.
- Y. S. Yang and M. X. Wan, *Journal of Materials Chemistry*, 2002, **12**, 897-901.
- S. J. He, X. W. Hu, S. L. Chen, H. Hu, M. Hanif and H. Q. Hou, *Journal of Materials Chemistry*, 2012, **22**, 5114-5120.
- D. Li, J. Huang and R. B. Kaner, *Accounts of Chemical Research*, 2009, **42**, 135-145.
- E. Marie, R. Rothe, M. Antonietti and K. Landfester, *Macromolecules*, 2003, **36**, 3967-3973.
- G. C. Li, S. P. Pang, G. W. Xie, Z. B. Wang, H. R. Peng and Z. K. Zhang, *Polymer*, 2006, **47**, 1456-1459.
- H. Tsutsumi, S. Fukuzawa, M. Ishikawa, M. Morita and Y. Matsuda, *Journal of the Electrochemical Society*, 1995, **142**, L168-L170.
- J.-W. Jeon, Y. Ma, J. F. Mike, L. Shao, P. B. Balbuena and J. L. Lutkenhaus, *Physical Chemistry Chemical Physics*, 2013, **15**, 9654-9662.
- R. V. Parthasarathy and C. R. Martin, *Chemistry of Materials*, 1994, **6**, 1627-1632.
- I. Lee, H. Il Park, S. Park, M. J. Kim and M. Yun, *Nano*, 2008, **3**, 75-82.
- J. M. McGraw, C. S. Bahn, P. A. Parilla, J. D. Perkins, D. W. Readey and D. S. Ginley, *Electrochimica Acta*, 1999, **45**, 187-196.
- R. Baddour, J. P. Pereiramos, R. Messina and J. Perichon, *Journal of Electroanalytical Chemistry*, 1991, **314**, 81-101.
- Y. Wang and G. Cao, *Advanced Materials*, 2008, **20**, 2251-2269.
- S. D. Perera, B. Patel, N. Nijem, K. Roodenko, O. Seitz, J. P. Ferraris, Y. J. Chabal and K. J. Balkus, Jr., *Advanced Energy Materials*, 2011, **1**, 936-945.
- F. Leroux, G. Goward, W. P. Power and L. F. Nazar, *Journal of the Electrochemical Society*, 1997, **144**, 3886-3895.
- M. Sathiya, A. S. Prakash, K. Ramesha, J. M. Tarascon and A. K. Shukla, *Journal of the American Chemical Society*, 2011, **133**, 16291-16299.
- S. Kuwabata, T. Idzu, C. R. Martin and H. Yoneyama, *Journal of the Electrochemical Society*, 1998, **145**, 2707-2710.
- F. Huguenin, M. Ferreira, V. Zucolotto, F. C. Nart, R. M. Torresi and O. N. Oliveira, *Chemistry of Materials*, 2004, **16**, 2293-2299.
- S. W. Lee, J. Kim, S. Chen, P. T. Hammond and Y. Shao-Horn, *ACS Nano*, 2010, **4**, 3889-3896.
- S. W. Lee, N. Yabuuchi, B. M. Gallant, S. Chen, B.-S. Kim, P. T. Hammond and Y. Shao-Horn, *Nature Nanotechnology*, 2010, **5**, 531-537.
- H. R. Byon, S. W. Lee, S. Chen, P. T. Hammond and Y. Shao-Horn, *Carbon*, 2011, **49**, 457-467.
- M. N. Hyder, S. W. Lee, F. C. Cebeci, D. J. Schmidt, Y. Shao-Horn and P. T. Hammond, *ACS Nano*, 2011, **5**, 8552-8561.
- L. Shao, J. W. Jeon and J. L. Lutkenhaus, *Chemistry of Materials*, 2012, **24**, 181-189.
- L. Shao, J.-W. Jeon and J. L. Lutkenhaus, *Journal of Materials Chemistry A*, 2013.
- G. Decher and J.-D. Hong, *Makromolekulare Chemie. Macromolecular Symposia*, 1991, **46**, 321-327.
- G. Decher, *Science*, 1997, **277**, 1232-1237.
- J. B. Schlenoff, S. T. Dubas and T. Farhat, *Langmuir*, 2000, **16**, 9968-9969.
- K. C. Krogman, N. S. Zacharia, S. Schroeder and P. T. Hammond, *Langmuir*, 2007, **23**, 3137-3141.
- T. Otto, P. Mundra, M. Schelter, E. Frolova, D. Dorfs, N. Gaponik and A. Eychmuller, *Chemphyschem*, 2012, **13**, 2128-2132.
- S. Y. Kim, J. Hong, R. Kaviani, S. W. Lee, M. N. Hyder, Y. Shao-Horn and P. T. Hammond, *Energy & Environmental Science*, 2013, **6**, 888-897.
- G. M. Nogueira, D. Banerjee, R. E. Cohen and M. F. Rubner, *Langmuir*, 2011, **27**, 7860-7867.
- B. N. Wang, D. Olmeijer, R. Shah and K. C. Krogman, in *Surface Innovations*, 2013, pp. 92-97.
- Y. F. Lin, C. H. Chen, W. J. Xie, S. H. Yang, C. S. Hsu, M. T. Lin and W. B. Jian, *ACS Nano*, 2011, **5**, 1541-1548.
- J. F. Qiang, Z. H. Yu, H. C. Wu and D. Q. Yun, *Synthetic Metals*, 2008, **158**, 544-547.
- J. Livage, *Chemistry of Materials*, 1991, **3**, 578-593.
- O. Pelletier, P. Davidson, C. Bourgaux, C. Coulon, S. Regnault and J. Livage, *Langmuir*, 2000, **16**, 5295-5303.
- K. C. Wood, N. S. Zacharia, D. J. Schmidt, S. N. Wrightman, B. J. Andaya and P. T. Hammond, *Proceedings of the National Academy of Sciences of the United States of America*, 2008, **105**, 2280-2285.
- L. Shao, J. W. Jeon and J. L. Lutkenhaus, *Journal of Materials Chemistry A*, 2013, **1**, 7648-7656.
- J. H. Cheung, W. B. Stockton and M. F. Rubner, *Macromolecules*, 1997, **30**, 2712-2716.
- W. D. Mulhearn, D. D. Kim, Y. Gu and D. Lee, *Soft Matter*, 2012, **8**, 10419-10427.
- S. Srinivasan and P. Pramanik, *Synthetic Metals*, 1994, **63**, 199-204.
- A. A. Akl, *Journal of Physics and Chemistry of Solids*, 2010, **71**, 223-229.
- Y. L. Cheah, N. Gupta, S. S. Pramana, V. Aravindan, G. Wee and M. Srinivasan, *Journal of Power Sources*, 2011, **196**, 6465-6472.
- P. J. Hung, K. H. Chang, Y. F. Lee, C. C. Hu and K. M. Lin, *Electrochimica Acta*, 2010, **55**, 6015-6021.
- C.-C. Hu and C.-H. Chu, *Journal of Electroanalytical Chemistry*, 2001, **503**, 105-116.



80x27mm (300 x 300 DPI)